

# Rotating Accelerator-Mode Islands

Oded Barash and Itzhack Dana

*Minerva Center and Department of Physics,  
Bar-Ilan University, Ramat-Gan 52900, Israel*

## Abstract

The existence of rotating accelerator-mode islands (RAIs), performing quasiregular motion in rotational resonances of order  $m > 1$  of the standard map, is firmly established by an accurate numerical analysis of all the known data. It is found that many accelerator-mode islands for relatively small nonintegrability parameter  $K$  are RAIs visiting resonances of different orders  $m \leq 3$ . For sufficiently large  $K$ , one finds also “pure” RAIs visiting only resonances of the *same* order,  $m = 2$  or  $m = 3$ . RAIs, even quite small ones, are shown to exhibit sufficient stickiness to produce an anomalous chaotic transport. The RAIs are basically different in nature from accelerator-mode islands in resonances of the “forced” standard map which was extensively studied recently in the context of quantum accelerator modes.

PACS numbers: 05.45.Ac, 45.05.+x, 05.45.Mt

## I. INTRODUCTION

During the last three decades, the classical concept of “accelerator mode” (AM) has become of central importance in the theory of chaotic transport in Hamiltonian systems [1, 2, 3, 4, 5, 6, 7, 8, 9, 10, 11, 12, 13, 14, 15, 16, 17]. Recently, this concept has also provided an illuminating explanation [18, 19, 20] for a purely quantum acceleration of kicked atoms falling under gravity, observed in atom-optics experiments [21]. AMs are generalized periodic orbits (POs) of Hamiltonian maps having a translational symmetry in phase space. A paradigmatic example is the standard map [1]

$$M : \quad p_{t+1} = p_t + K \sin(x_t), \quad x_{t+1} = x_t + p_{t+1} \bmod(2\pi), \quad (1)$$

where  $p$  is angular momentum,  $x$  is angle,  $K$  is a nonintegrability parameter, and  $t$  is the “integer” time. The map (1) and its orbit structure are translationally invariant in  $p$  with period  $2\pi$  on the cylindrical phase space  $-\infty < p < \infty$ ,  $0 \leq x < 2\pi$ . This allows to define consistently a PO of (minimal) period  $n$  of (1) in a generalized fashion:

$$p_{t+n} = p_t + 2\pi w, \quad x_{t+n} = x_t, \quad (2)$$

where  $w$  is an integer, the “jumping index”. For  $w = 0$ , (2) corresponds to a usual (closed) PO on the cylinder while for  $w \neq 0$  the PO is an AM with average acceleration  $2\pi w/n$  per map iteration. If the AM is stable, its  $n$  points are surrounded by islands. Stickiness to the boundaries of AM islands can lead to a superdiffusion of the chaotic motion,  $\langle p_t^2 \rangle \propto t^\mu$ ,  $1 < \mu < 2$  [8, 9, 10, 11, 12, 13], where  $\langle \rangle$  denotes ensemble average in the chaotic region.

AMs can arise only for sufficiently large  $K$ ,  $K > K_c \approx 0.9716$ , when no rotational tori exist [22] and unbounded motion in the  $p$  direction becomes then possible. Thus, AM islands are basically different in nature from the well-known rotational-resonance islands which exist for arbitrarily small  $K$ . The latter islands form the most basic component of ordered and stable motion in the twist map (1). They are associated with the closed ( $w = 0$ ) “Poincaré-Birkhoff” or “ordered” POs [23, 24] which are dynamically equivalent to pure rotations, i.e., the  $K = 0$  POs, and emerge from them as  $K$  is “switched on” [23]. Despite the difference above, however, one may expect from the following general arguments the existence of an interesting kind of AM islands, resembling rotational-resonance islands

in some aspects.

It is known [25] that rotational resonances for the standard map (and similar maps [26, 27]) can be constructed in a well-defined way for *all*  $K$ ; a resonance of order  $m$  is a chain of  $m$  “zones” built on a hyperbolic ordered PO of period  $m$  (see more details in Sec. II). Strong numerical evidence [25] and exact results [26, 28] indicate that for  $K > K_c$  the resonances so constructed give a *partition* of phase space. This implies that an arbitrary orbit of (1) consists of *quasiregular* segments within resonances, where each segment is a piece of the orbit performing a number of rotations in one resonance [29, 30]. Now, a general stability island must lie entirely in some resonance zone [17] and will thus perform a similar quasiregular motion within resonances. Clearly, the rotational quasiregularity is evident *only* when the island visits resonances of order  $m > 1$ . AM islands visiting  $m > 1$  resonances are most interesting objects since they exhibit a “hybrid” nature: In some time intervals, they rotate like  $m > 1$  resonance islands in a near-integrable regime ( $K \ll 1$ ) and at other times they accelerate due to particular transitions between resonances occurring only for  $K > K_c$ . We thus call these islands, if they exist, “rotating accelerator-mode islands” (RAIs). The RAIs should have a distinct impact on Hamiltonian transport by generating a new kind of chaotic flight, featuring a quasiregular steplike structure due to the “horizontal” rotation within resonances. General ideas in Ref. [17] were illustrated only for the most well-known AM islands of the standard map, those with central period  $n = 1$  which emerge for  $K > 2\pi$  [1, 3, 4]. These islands lie within  $m = 1$  resonances [17]. The question of the actual existence of RAIs was not addressed in Ref. [17].

In this paper, the existence of RAIs in the standard map is firmly established by an accurate numerical analysis, examining also all the known data on AM islands of which we are aware. In this analysis, the sequence of resonances visited by an orbit is determined by using the efficient method introduced in work [30]. A large fraction of the AM islands for  $K < 2\pi$ , listed in Ref. [4], are found to be RAIs visiting resonances of different orders  $m \leq 3$ . Some of the significant peaks in the chaotic-diffusion coefficient observed in Ref. [4] for  $K < 2\pi$  are due to RAIs. Among all the period-2 AM islands for  $2\pi < K < 20$ , listed in Ref. [3], we have found RAIs visiting resonances of the *same* order  $m = 2$  (“pure”  $m = 2$  RAIs). We discover at  $K \approx 8.916$  an apparently new AM island, a pure  $m = 3$

RAI. It is shown that even quite small RAIs exhibit sufficient stickiness to produce an anomalous chaotic transport. Due to limitations in our available computational resources, we were not able to find RAIs visiting resonances of order  $m > 3$ . The paper is organized as follows. In Sec. II, we briefly summarize the notion of rotational quasiregularity within resonances. In Sec. III, the existence of RAIs is established by an accurate determination of the quasiregularity characteristics of many AM islands. In Sec. IV, we briefly study some of the effects of RAIs on Hamiltonian chaotic transport. A discussion and conclusions are presented in Sec. V, where we also consider the basic difference between RAIs and AM islands visiting resonances of the “forced” standard map [map (1) with the addition of a constant force], which has attracted much attention recently in the context of “quantum AMs” [18, 19, 20, 21].

## II. ROTATIONAL RESONANCES AND QUASIREGULARITY

We briefly summarize here the definition of rotational resonances for the standard map [25] and the notion of quasiregularity within these resonances [17, 29, 30]. Let us first recall the concept of rotationally *ordered* POs [24]. In the pure-rotation case of  $K = 0$ , with constant  $p_t = p_0$ , the sequence of orbit angles  $x_t$  is given by  $x_t = x_0 + p_0 t \bmod(2\pi)$ . For rational winding number  $\nu = p_0/(2\pi) = l/m$ , where  $(l, m)$  are coprime integers, the orbit must be a PO with period  $m$ ; the  $m$  PO points are uniformly distributed on the circle  $[0, 2\pi)$ , i.e., the “gap”  $\mathbf{G}_t$  between  $x_t$  and a neighboring point has the constant width  $2\pi/m$ , independent of  $t$ . The rotational motion on the circle is expressed by the fact that  $\mathbf{G}_{t+1}$  is also a gap, always separated from  $\mathbf{G}_t$  by  $|l| - 1$  gaps. Now, for  $K \neq 0$ , the winding number  $\nu$  for a closed ( $w = 0$ ) PO is the average value of  $p_t/(2\pi)$  and  $\nu$  is again rational. A gap is a pair of PO points having neighboring values of  $x_t$  in the circle. Then, a rotationally ordered PO is a closed PO having the two main characteristics of a  $K = 0$  PO: (a)  $\nu = l/m$ , where  $m$  is the PO period and  $(l, m)$  are coprime. (b) If  $\mathbf{G}_t$  is a gap,  $\mathbf{G}_{t+1}$  is also a gap, always separated from  $\mathbf{G}_t$  by  $|l| - 1$  gaps. Unlike the case of  $K = 0$ , however, the gap width generally depends on  $t$ .

An ordered hyperbolic PO with arbitrary winding number  $\nu = l/m$  exists for all  $K$  [24]. One gap of this PO, say  $\mathbf{G}_0$ , appears to be always symmetrically positioned around the

“dominant” symmetry line  $x = \pi$ , i.e.,  $\pi - x_L = x_R - \pi$ , where  $L$  and  $R$  denote the left and right point, respectively, of  $\mathbf{G}_0$ . The  $l/m$  resonance is now defined, briefly, as follows (see more details in Refs. [17, 25] and refer to the examples in Fig. 1). One constructs in  $\mathbf{G}_0$  a closed region  $\mathcal{Z}^{(0)}(l/m)$  bounded by four curved segments, which are suitably chosen pieces of the stable and unstable manifolds of  $L$  and  $R$  under the map  $M^m$ . The  $l/m$  resonance is then the chain of  $m$  zones  $\mathcal{Z}^{(t)}(l/m) = M^{-t}\mathcal{Z}^{(0)}(l/m)$ ,  $t = 0, \dots, m - 1$ ; see, e.g., resonances  $0/1$  and  $1/2$  in Fig. 1. Clearly, the zone  $\mathcal{Z}^{(m)}(l/m) = M^{-m}\mathcal{Z}^{(0)}(l/m)$  lies again in  $\mathbf{G}_0$  and differs from the “principal” zone  $\mathcal{Z}^{(0)}(l/m)$  by two *turnstile*s created by homoclinic oscillations under  $M^{-m}$  (the dashed lines in Fig. 1). Each turnstile consists of two lobes of equal area. By construction, the lobes outside (inside)  $\mathcal{Z}^{(0)}(l/m)$  form the region entering (exiting) resonance  $l/m$  in one iteration of  $M$ .

Strong numerical evidence [25, 30] and exact results [26, 28] indicate that for  $K > K_c \approx 0.9716$  the resonances constructed as above give, for all  $l/m$ , a complete partition of phase space. This implies that a generic orbit must have all its points within resonances and must therefore perform a quasiregular motion as follows. An initial orbit point in, say, resonance  $l/m$  will “rotate”, jumping from zone  $\mathcal{Z}^{(t)}(l/m)$  in gap  $\mathbf{G}_t$  to zone  $\mathcal{Z}^{(t+1)}(l/m)$  in gap  $\mathbf{G}_{t+1}$ , until it will arrive to  $\mathcal{Z}^{(0)}(l/m)$ . If it does not lie in an exiting turnstile lobe, it will rotate again, returning to  $\mathcal{Z}^{(0)}(l/m)$  after  $m$  iterations. If, on the other hand, it lies in an exiting turnstile lobe, more precisely in the *overlap* of this lobe with an entering turnstile lobe of resonance  $l'/m'$  (such overlaps are the shaded regions in Fig. 1), it will escape to zone  $\mathcal{Z}^{(m'-1)}(l'/m')$  of  $l'/m'$ ; it will then perform at least a finite number of rotations (of  $m'$  iterations each) in  $l'/m'$  before escaping to another resonance. Thus, the orbit is a sequence of quasiregular segments, each lying in some resonance  $l_r/m_r$ ,  $-\infty < r < \infty$ , and having a length of  $q_r m_r$  iterations, where  $q_r$  is the number of rotations performed in  $l_r/m_r$ . We then say that the orbit is of quasiregularity *type*  $\tau = \dots, (l_r/m_r)_{q_r}, (l_{r+1}/m_{r+1})_{q_{r+1}} \dots$  [29, 30]. As an example, Fig. 1 shows five orbit points, labeled by  $t = 1, \dots, 5$ , in two consecutive quasiregular segments  $(0/1)_3, (1/2)_1$ .

In the case that the orbit is a PO, i.e., it satisfies (2), its type can be written in a more compact form [17, 29]. Clearly, a PO can visit only a finite number ( $d$ ) of resonances on the torus  $0 \leq x, p < 2\pi$  [by taking also  $p_t$  modulo  $2\pi$  in (1)]. Thus, on

the cylinder, it will generally visit a set of  $d$  resonances  $\{l_r/m_r\}_{r=1}^d$  and all the translates  $\{l_r/m_r + bw_\tau\}_{r=1}^d$  of this set in the  $p$ -direction, where  $b$  takes all the integer values and  $w_\tau$  is some integer related to  $w$ , see below. The type  $\tau$  of the PO must be then essentially the repetition of a “block”  $\Gamma$ ,  $\tau = \dots, \Gamma(-w_\tau), \Gamma(0), \Gamma(w_\tau), \Gamma(2w_\tau), \dots$ , where  $\Gamma(bw_\tau) = (l_1/m_1 + bw_\tau)_{q_1}, \dots, (l_d/m_d + bw_\tau)_{q_d}$ . If the periodic cycle is completed exactly after visiting one block, one has  $w = w_\tau$  and the period  $n = n_\tau = \sum_{r=1}^d q_r m_r$ . Generally, however, the periodic cycle is completed only after visiting more than one block, say  $c$  blocks. Then,  $w = cw_\tau$  and  $n = cn_\tau$ . The type  $\tau$  of the PO will be thus specified by  $(\Gamma; w_\tau, c)$ , where  $\Gamma$  stands, e.g., for  $\Gamma(0)$ . The average acceleration per iteration is  $2\pi w/n = 2\pi w_\tau/n_\tau$ .

### III. ROTATING ACCELERATOR-MODE ISLANDS (RAIs)

If a period- $n$  PO is stable, each of its  $n$  points is the “center” of an island in a chain of  $n$  islands. As shown in Ref. [17], an island must lie entirely within the zone of some resonance  $l/m$ . If this zone is the principal one,  $\mathcal{Z}^{(0)}(l/m)$ , the island will be either outside the turnstiles or completely within the turnstile overlap (TO) of  $l/m$  with another resonance  $l'/m'$  [17]. Thus, the island will always lie entirely in the basic region [resonance zone (outside the turnstiles) or TO] where its center lies, so that one can characterize the island chain by the type  $(\Gamma; w_\tau, c)$  of its central PO. For example, the well-known period-1 AM islands arising for  $K > 2\pi|w|$  [1, 3, 4] must all lie within first-order ( $m = 1$ ) resonances and their type is  $\tau = ((0/1)_1; w, 1)$ ; this is because  $n = cn_\tau = c \sum_{r=1}^d q_r m_r$  implies, for  $n = 1$ , that  $c = d = q_1 = m_1 = 1$ . Since the fraction of phase space occupied by the  $m = 1$  resonances approaches 100% as  $K$  increases [25], and is already significant for  $K > K_c$ , it is natural to ask about the existence of RAIs, i.e., AM islands visiting resonances of order  $m > 1$ .

To answer this question, we have carefully examined all the data on standard-map AM islands of which we are aware. Most of this data appears in Refs. [3, 4, 14]; apparently new AM islands have been also considered. The type of an island chain or of its central PO was accurately determined by using the efficient method introduced in Ref. [30]. Briefly, this method is based on the fact, proven in Ref. [30], that one can always find a sawtooth

map  $M_s$  [i.e., the map (1) with  $\sin(x)$  replaced by a sawtooth function and with  $K$  replaced by a properly chosen parameter  $K_s$ ] such that for each orbit  $\mathcal{O}$  of  $M$  there exists an orbit  $\mathcal{O}_s$  of  $M_s$  visiting the *same* resonances as those visited by  $\mathcal{O}$ . Since the boundaries of the resonances of  $M_s$  are given by simple analytic expressions [26], this allows one to determine the type of  $\mathcal{O}$  without calculating the complicated resonance boundaries of  $M$ .

Our results are presented in Tables I and II. In Table I, we give the type  $\tau$  of many AM island chains for  $K_c < K < 2\pi$ . These chains, most of which appear in Table I in Ref. [4], were chosen in a well-defined and natural way, i.e., they have at least one island lying on  $p = 0$  (see also next section), except for chains no. 7, 8 which are given for future reference; initial conditions  $(x_0, p_0)$  within the islands are specified, as well as the values of  $K$ ,  $n$ , and  $w$ . We see that more than half of these island chains (no. 1-12, 15, 16), mostly at the smaller values of  $K$ , are RAIs visiting resonances of order  $m = 2$  and/or  $m = 3$ . The central PO for RAI no. 6, with  $n = 5$  and  $w = 1$ , consists of the five points shown in Fig. 1. As another example, we show in Fig. 2 the central PO for RAI no. 1, with  $n = 11$  and  $w = 1$ , together with the four resonances visited,  $l/m = 0/1, 1/3, 1/2, 2/3$ . RAI no. 5, with  $n = 10$ , emerges by period-doubling bifurcation from RAI no. 4 with  $n = 5$ . This is reflected in the fact that the types of RAIs no. 4 and 5 have the same basic block  $\Gamma$  but  $c = w = 2$  for RAI no. 5, in contrast with  $c = w = 1$  for RAI no. 4. Similarly, RAI no. 8, with  $n = 8$ , emerges by period-doubling bifurcation from RAI no. 7 with  $n = 4$ .

In Table II, we give the type  $\tau$  of AM islands with  $n = 1, 2, 3$  for  $2\pi < K < 20$ . Most of these islands, those with  $n = 1, 2$ , were selected from Table I in Ref. [3]. As in that work, we give in Table II the stability interval  $(K_1, K_2)$  of each island and corresponding initial conditions  $(x_0, p_0)$  for  $K = K_{1,2}$ ; the values of  $n$  and  $w$  are also shown. Islands no. 2, 6, and 9 emerge by period-doubling bifurcation from islands no. 1, 5, and 8, respectively. All these islands lie in  $m = 1$  resonances. The only AM islands that we were able to identify as RAIs in this  $K$  interval are no. 3, 4, and 7. These RAIs are “pure”, i.e., they visit resonances of the same order  $m = 2$  (RAIs no. 3 and 7) or  $m = 3$  (RAI no. 4). The latter RAI is apparently a new AM island. Figs. 3-5 show the central PO for each of these pure RAIs, together with the resonances visited and the turnstiles responsible for the transition from resonance  $1/m$  to resonance  $1/m + w$ ; this transition causes the acceleration.

RAIs can be very small islands. As examples, we show in Fig. 6 one island of each of the RAI chains to which we refer in Figs. 2-5.

#### IV. CHAOTIC TRANSPORT IN THE PRESENCE OF RAIs

We now briefly study the effect of RAIs on chaotic transport. Given an ensemble  $\mathcal{E}$  of initial conditions  $(x_0, p_0)$  in phase space for  $K > K_c$ , the transport of  $\mathcal{E}$  is usually measured by the time evolution of  $\langle (p_t - p_0)^2 \rangle_{\mathcal{E}}$ , where  $\langle \cdot \rangle_{\mathcal{E}}$  denotes average over  $\mathcal{E}$ . In the absence of AM islands, with  $\mathcal{E}$  lying entirely within the connected chaotic region,  $\langle (p_t - p_0)^2 \rangle_{\mathcal{E}} \approx 2Dt$  for large  $t$ , where  $D$  is the chaotic-diffusion coefficient [1]. In Ref. [4],  $\mathcal{E}$  was naturally chosen as a physical ensemble of well-defined angular momentum  $p = p_0$ ,  $0 \leq x_0 < 2\pi$ , and the quantity  $D_{\mathcal{E},t}(K) = \langle (p_t - p_0)^2 \rangle_{\mathcal{E}} / (2t)$  was calculated at fixed large  $t$  as a function of  $K$ , for  $K_c < K < 2\pi$ . Whenever an AM island crosses the line  $p = p_0$  as  $K$  is varied,  $D_{\mathcal{E},t}(K)$  exhibits “ballistic” peaks, see Fig. 7 for  $p_0 = 0$  and Ref. [4]. The AM islands on  $p = 0$  in Table I were determined in this way. Some of the most significant peaks in Fig. 7 are due to RAIs, e.g., RAIs no. 6-8, 10, 15, 16. In particular, the peak due to RAI no. 16 is relatively broad in  $K$ .

If  $\mathcal{E}$  is an ensemble lying entirely within the connected chaotic region and there exist AM islands exhibiting sufficient stickiness, one observes an anomalous, superdiffusive chaotic transport,  $\langle (p_t - p_0)^2 \rangle_{\mathcal{E}} \propto t^\mu$  with anomalous exponent  $\mu$ ,  $1 < \mu < 2$  [8, 9, 10, 11, 12, 13]. As far as we are aware, this anomalous transport in the standard map was observed only for AM islands whose central PO has period  $n = 1$  (such as islands no. 1, 5, and 8 in Table II) or satellites of these islands. All these islands lie in  $m = 1$  resonances and are not RAIs.

To show that RAIs affect chaotic transport, we consider, as a first example, the case of RAI no. 7 in Table I ( $K = 2.975$ ), see Fig. 8. The ensemble  $\mathcal{E}$  consists of the points  $(x_0, p_0)$  with  $p_0 = 0$  and  $x_0$  taking  $10^5$  values uniformly distributed in  $[0, 2\pi)$ . This ensemble is chaotic with the exception of  $\sim 20\%$  of it lying in ordinary (non-AM) islands within the 0/1 resonance. The only source of anomalous transport can be stickiness to the boundary of the RAI above, since no other AM islands seem to exist for  $K = 2.975$ . To verify that this RAI



boundary is indeed sticky, we have iterated the ensemble  $t = 10^4$  times and plotted only the points  $(x_{t'}, p_{t'} \bmod(2\pi))$ , for all  $t' \leq t$  and with  $p_{t'}/(2\pi) > 100$ ; since the RAI has central period  $n = 4$ ,  $p_{t'}/(2\pi)$  cannot be larger than  $t/4 = 2500$ . The results are shown in the inset of Fig. 8, and one can see a strong stickiness to the RAI boundary. As a consequence, we observe a clearly superdiffusive chaotic transport with anomalous exponent  $\mu \approx 1.28$ , see Fig. 9.

As other examples, we have considered the much smaller RAIs shown in Figs. 6(b), 6(c), and 6(d). To verify the stickiness to the boundary of these RAIs, we first chose  $\mathcal{E}$  as a chaotic ensemble in the close neighborhood of the RAI, see details in the captions of Figs. 6 and 10. The time evolution of  $\langle p_t - p_0 \rangle_{\mathcal{E}} / (2\pi)$  was then calculated for sufficiently large  $t$ ; the results are shown in Fig. 10. We see that in a significant time interval (e.g.,  $t \leq 100$  in Fig. 10(b)),  $\langle p_t - p_0 \rangle_{\mathcal{E}} / (2\pi)$  evolves essentially as if  $\mathcal{E}$  were concentrated inside the RAI, i.e., it exhibits the steplike structure due to rotation in  $m = 2$  resonances (see inset of Figs. 10(a) and 10(c)) or in  $m = 3$  resonances (see inset of Figs. 10(b)) and its initial average slope is  $\sim w/n$ . This is clear evidence for stickiness to the RAI boundary, leading to chaotic flights. In the course of time, more and more points of the ensemble leave the RAI boundary and enter the chaotic region. Then,  $\langle p_t - p_0 \rangle_{\mathcal{E}} / (2\pi)$  starts to saturate around some constant value which should correspond to the center of a Gaussian distribution describing normal chaotic diffusion. The saturation value of  $\langle p_t - p_0 \rangle_{\mathcal{E}} / (2\pi)$  in Fig. 10(c) is much larger than that in Figs. 10(a) and 10(b) due to the relatively large value of  $w/n = 1$  and to the much stronger stickiness, as one can see by comparing Fig. 6(d) with Figs. 6(b) and 6(c).

## V. DISCUSSION AND CONCLUSIONS

In this paper, we have established the existence of a most interesting kind of stability island in the standard map, the RAI, exhibiting two diametrically opposite dynamical behaviors: The rotational motion, characteristic of the integrable ( $K = 0$ ) case, and the acceleration which emerges only in the global-chaos regime of  $K > K_c \approx 0.9716$ . As indicated by Table I, RAIs appear to be abundant for sufficiently small  $K > K_c$  but they also exist in strong-chaos regimes (Table II), where  $m > 1$  resonances are quite small and essentially all phase space is occupied by  $m = 1$  resonances. For large  $K > 2\pi$ , it is

possible to have turnstile overlap between resonances of the same order, e.g., resonances  $1/m$  and  $1/m + w$ , and pure RAIs can then arise, see Figs. 3-5. If the map (1) is restricted to the torus  $T^2 : 0 \leq x, p < 2\pi$ , by taking also  $p_t$  modulo  $2\pi$ , pure RAIs look precisely like rotational-resonance islands in a near-integrable regime ( $K \ll 1$ ). Stickiness to the boundary of RAIs, especially of pure RAIs, leads to chaotic flights featuring a quasiregular steplike structure due to the rotational motion within resonances, see Fig. 10. Such a quasiregular structure was observed recently [15] in the weak-chaos regime of a perturbed pseudochaotic map. We have shown here that it also occurs in strong-chaos regimes. It would be most interesting if one could establish the existence of pure RAIs of arbitrarily large order  $m$ . Such RAIs may give rise to chaotic flights with arbitrarily long quasiregular steps; these flights were shown to be possible for the system studied in Ref. [15].

There has been much interest recently [18, 19, 20] in the forced standard map

$$M_\Omega : \quad p_{t+1} = p_t + K \sin(x_t) + 2\pi\Omega, \quad x_{t+1} = x_t + p_{t+1} \bmod(2\pi), \quad (3)$$

where  $\Omega$  is a constant “force”. It was shown [18] that  $M_\Omega$  provides an approximate description of the vicinity of quantum resonance for a periodically kicked particle in the presence of gravity. The quantum resonant behavior of this system manifests itself in the so-called quantum AMs [21] which correspond to classical AM islands of  $M_\Omega$ . The map (3) arises and was studied also in other contexts [31, 32]. It is instructive to compare some AM islands of (3) with the RAIs in the standard map ( $\Omega = 0$ ). Consider, for simplicity, the case of integer  $\Omega \neq 0$  (the arguments and conclusions below can be easily extended to the case of general rational  $\Omega$ ). In this case,  $M_\Omega$  and the standard map obviously coincide if both maps are restricted to the basic torus  $T^2$ . Thus, for sufficiently small  $K$ , there exist rotational-resonance islands in any resonance  $l/m$  of  $M_\Omega$  on  $T^2$ . On the cylinder, such an island will correspond to an AM island: In one iteration of (3), the island in zone  $\mathcal{Z}^{(t)}(l/m)$ ,  $t = 0, \dots, m - 1$ , will accelerate by jumping to zone  $\mathcal{Z}^{(t+1)}(l/m + \Omega)$  of resonance  $l/m + \Omega$ . Clearly, this behavior is basically different from that of, say a pure RAI, which *remains* (rotates) in resonance  $l/m$  for  $m$  (or a multiple of  $m$ ) iterations before jumping to resonance  $l/m + w$ . The rotational motion of RAIs, combined with acceleration, is *not* featured by the AM islands above of  $M_\Omega$ . It would be therefore interesting to study the fingerprints of RAIs in the quantized standard map.

## ACKNOWLEDGMENTS

This work was partially supported by the Israel Science Foundation (Grant No. 118/05).

---

- [1] B.V. Chirikov, Phys. Rep. **52**, 263 (1979).
- [2] J.R. Cary and J.D. Meiss, Phys. Rev. A **24**, 2664 (1981).
- [3] C.F.F. Karney, A.B. Rechester, and R.B. White, Physica (Amsterdam) **4D**, 425 (1982).
- [4] Y.H. Ichikawa, T. Kamimura, and T. Hatori, Physica (Amsterdam) **29D**, 247 (1987).
- [5] I. Dana, Physica (Amsterdam) **39D**, 205 (1989).
- [6] H.T. Kook and J.D. Meiss, Phys. Rev. A **41**, 4143 (1990).
- [7] I. Dana and T. Horesh, Lecture Notes in Physics **511**, 51 (1998).
- [8] R. Ishizaki, T. Horita, T. Kobayashi, and H. Mori, Prog. Theor. Phys. **85**, 1013 (1991).
- [9] G.M. Zaslavsky, M. Edelman, and B.A. Niyazov, Chaos **7**, 159 (1997).
- [10] S. Benkadda, S. Kassibrakis, R. White, and G. Zaslavsky, Phys. Rev. E **55**, 4909 (1997).
- [11] R.B. White, S. Benkadda, S. Kassibrakis, and G.M. Zaslavsky, Chaos **8**, 757 (1998).
- [12] G.M. Zaslavsky and M. Edelman, Chaos **10**, 135 (2000).
- [13] G.M. Zaslavsky, Phys. Rep. **371**, 461 (2002), and references therein.
- [14] S. Saito, K. Hirose, and Y.H. Ichikawa, Chaos, Solitons, and Fractals **11**, 1433 (2000), and references therein.
- [15] I. Dana, Phys. Rev. E **69**, 016212 (2004).
- [16] V. Rom-Kedar and G. Zaslavsky, Chaos **9**, 697 (1999), and references therein.
- [17] O. Barash and I. Dana, Phys. Rev. E **71**, 036222 (2005).
- [18] S. Fishman, I. Guarneri, and L. Rebuzzini, Phys. Rev. Lett. **89**, 084101 (2002); J. Stat. Phys. **110**, 911 (2003).
- [19] A. Buchleitner, M.B. d’Arcy, S. Fishman, S.A. Gardiner, I. Guarneri, Y.-Z. Ma, L. Rebuzzini, and G.S. Summy, Phys. Rev. Lett. **96**, 164101 (2006).
- [20] I. Guarneri, L. Rebuzzini, and S. Fishman, Nonlinearity **19**, 1141 (2006).
- [21] R.M. Godun *et al.*, Phys. Rev. A **62**, 013411 (2000); M.B. d’Arcy *et al.*, Phys. Rev. E **64**, 056233 (2001); S. Schlunk *et al.*, Phys. Rev. Lett. **90**, 054101 (2003); *ibid.*, 124102 (2003); Z.-Y. Ma, M.B. d’Arcy, and S.A. Gardiner, Phys. Rev. Lett. **93**, 164101 (2004).

- [22] J.M. Greene, *J. Math. Phys.* **20**, 1183 (1979).
- [23] A.J. Lichtenberg and M.A. Lieberman, *Regular and Chaotic Dynamics* (Springer-Verlag, Berlin, 1992).
- [24] J.D. Meiss, *Rev. Mod. Phys.* **64**, 795 (1992), and references therein.
- [25] R.S. MacKay, J.D. Meiss, and I.C. Percival, *Physica (Amsterdam)* **27D**, 1 (1987), and references therein.
- [26] Q. Chen, I. Dana, J.D. Meiss, N.W. Murray, and I.C. Percival, *Physica (Amsterdam)* **46D**, 217 (1990).
- [27] O. Barash and I. Dana, *Phys. Rev. E* **74**, 056202 (2006).
- [28] Q. Chen, *Phys. Lett. A* **123**, 444 (1987).
- [29] I. Dana, *Phys. Rev. Lett.* **64**, 2339 (1990).
- [30] I. Dana, *Phys. Rev. Lett.* **70**, 2387 (1993), and references therein.
- [31] A.T. Filippov and Yu. S. Gal'pern, *Phys. Lett. A* **172**, 471 (1993).
- [32] R. Ishizaki and H. Mori, *Prog. Theor. Phys.* **97**, 201 (1997); *ibid.*, **100**, 1131 (1998).

Table I. Quasiregularity type  $\tau = (\Gamma; w_\tau, c)$  of AM island chains for  $K_c < K < 2\pi$ . The period  $n$ , jumping index  $w$ , and initial conditions  $(x_0, p_0)$  are also shown.

	$K$	$\tau = (\Gamma; w_\tau, c)$	$n$	$w$	$(x_0, p_0)/(2\pi)$
1	2.1834	$((0/1)_3, (1/3)_1, (1/2)_1, (2/3)_1; 1, 1)$	11	1	(0.097, 0.0)
2	2.374	$((0/1)_3, (1/2)_1; 1, 1)$	7	1	(0.1085, 0.0)
3	2.55097	$((0/1)_4, (1/2)_1, (1/1)_3, (3/2)_1; 2, 1)$	11	2	(0.102632, 0.0)
4	2.5875	$((0/1)_3, (1/2)_1; 1, 1)$	5	1	(0.098, 0.0)
5	2.58867	$((0/1)_3, (1/2)_1; 1, 2)$	10	2	(0.099, 0.00151)
6	2.63894	$((0/1)_3, (1/2)_1; 1, 1)$	5	1	(0.105, 0.0)
7	2.975	$((0/1)_2, (1/2)_1; 1, 1)$	4	1	(0.33445, 0.4)
8	2.9845	$((0/1)_2, (1/2)_1; 1, 2)$	8	2	(0.344, 0.412)
9	3.34579	$((0/1)_9, (1/2)_1; 1, 1)$	11	1	(0.3851, 0.0)
10	3.50287	$((0/1)_5, (1/2)_1; 1, 1)$	7	1	(0.64, 0.0)
11	3.61283	$((0/1)_9, (1/3)_1, (1/1)_2, (5/3)_1; 2, 1)$	17	2	(0.336347, 0.0)
12	3.76991	$((0/1)_5, (1/2)_1; 1, 1)$	7	1	(0.6195, 0.0)
13	3.78247	$((0/1)_3, (1/1)_2; 2, 1)$	5	2	(0.0667, 0.0)
14	3.80761	$((0/1)_3, (1/1)_2; 2, 1)$	5	2	(0.07, 0.0)
15	4.141	$((0/1)_1, (1/2)_1; 1, 1)$	3	1	(0.285, 0.0)
16	4.66526	$((0/1)_1, (1/2)_1; 1, 1)$	3	1	(0.34805, 0.0)
17	5.02654	$((0/1)_3, (1/1)_1, (2/1)_2, (3/1)_1; 4, 1)$	7	4	(0.04432, 0.0)
18	5.12079	$((0/1)_2, (1/1)_1; 2, 1)$	3	2	(0.277, 0.0)
19	5.32499	$((0/1)_3, (1/1)_2; 2, 1)$	4	2	(0.055, 0.0)
20	5.41924	$((0/1)_2, (1/1)_2, (2/1)_1; 3, 1)$	5	3	(0.338162, 0.0)
21	5.45066	$((0/1)_2, (1/1)_1; 2, 2)$	6	4	(0.22265, 0.0)
22	5.51663	$((0/1)_2, (1/1)_1; 2, 1)$	3	2	(0.334, 0.0)
23	5.79623	$((0/1)_6, (1/1)_1; 2, 1)$	7	2	(0.3255, 0.0)
24	6.173229	$((0/1)_3, (1/1)_1, (2/1)_1, (3/1)_1; 4, 1)$	6	4	(0.0286, 0.0)

Table II. Quasiregularity type  $\tau = (\Gamma; w_\tau, c)$  of AM island chains for  $2\pi < K < 20$ . Also shown are the period  $n$ , the jumping index  $w$ , and the stability interval  $(K_1, K_2)$  of the island chain with corresponding initial conditions  $(x_0, p_0)$  for  $K = K_{1,2}$ .

	$\tau = (\Gamma; w_\tau, c)$	$n$	$w$	$K_1$	$(x_0, p_0)/(2\pi), K = K_1$	$K_2$	$(x_0, p_0)/(2\pi), K = K_2$
1	$((0/1)_1; 1, 1)$	1	1	6.28319	(0.2500, 0.0)	7.44840	(0.34059, 0.0)
2	$((0/1)_1; 1, 2)$	2	2	7.44840	(0.34059, 0.0)	7.71340	(0.3845, 0.0928)
3	$((1/2)_1; 1, 1)$	2	1	8.67893	(0.27999, 0.321577)	8.68826	(0.28696, 0.32717)
4	$((1/3)_1; 1, 1)$	3	1	8.91596	(0.934594, 0.6522)	8.91603	(0.934641, 0.651819)
5	$((0/1)_1; 2, 1)$	1	2	12.56638	(0.2500, 0.0)	13.1876	(0.2990, 0.0)
6	$((0/1)_1; 2, 2)$	2	4	13.1876	(0.2990, 0.0)	13.33848	(0.3233, 0.0494)
7	$((1/2)_1; 2, 1)$	2	2	15.2394	(0.268606, 0.295564)	15.24126	(0.270938, 0.29762)
8	$((0/1)_1; 3, 1)$	1	3	18.84956	(0.2500, 0.0)	19.26929	(0.2832, 0.0)
9	$((0/1)_1; 3, 2)$	2	6	19.26929	(0.2832, 0.0)	19.3728	(0.2998, 0.0333)

## FIGURE CAPTIONS

Fig. 1. Solid lines: Resonances  $0/1$  (region  $LERF$ ) and  $1/2$  (with principal zone  $L'E'R'F'$ ) for  $K = 2.63894$ . The dashed-line segments  $FBH$  and  $GAE$  form, together with the corresponding solid-line segments, the lower and upper turnstile, respectively, of  $0/1$ ; similarly for the turnstiles of  $1/2$ . The shaded regions are the overlaps of the upper turnstile of  $0/1$  with the lower turnstile of  $1/2$ . Also shown are five orbit points labeled by the time index  $t = 1, \dots, 5$ . Since point 3 lies in  $0/1$  within a turnstile overlap, its iterate (point 4) lies in zone 1 of  $1/2$ .

Fig. 2. Regions bounded by solid lines: Resonances  $0/1$ ,  $1/3$ ,  $1/2$ , and  $2/3$  (in ascending order) for  $K = 2.1834$ . The dashed lines define the resonance turnstiles. The points (filled circles) give the central PO of the AM island chain no. 1 in Table I; this is a RAI chain. The arrow indicates a point to which we shall refer in the caption of Fig. 6.

Fig. 3. Regions bounded by solid lines: Resonances  $1/2$  and  $3/2$  for  $K = 8.68$ . The dashed lines define the resonance turnstiles. The four points, labeled by the time index  $t = 1, \dots, 4$ , give the central PO and its iterate for the AM island chain no. 3 in Table II; this is a pure RAI chain.

Fig. 4. Regions bounded by solid lines: Resonances  $1/3$  and  $4/3$  for  $K = 8.916$ . The dashed lines define the resonance turnstiles. The six points, labeled by the time index  $t = 1, \dots, 6$ , give the central PO and its iterate for the AM island chain no. 4 in Table II; this is a pure RAI chain.

Fig. 5. Regions bounded by solid lines: Resonances  $1/2$ ,  $3/2$ , and  $5/2$  for  $K = 15.24035$ . The dashed lines define the resonance turnstiles. The four points, labeled by the time index  $t = 1, \dots, 4$ , give the central PO and its iterate for the AM island chain no. 7 in Table II; this is a pure RAI chain. Point 2 in  $1/2$  is mapped into point 3 in  $5/2$  by turnstile overlap, “jumping over”  $3/2$ ; this leads to  $w = 2$ .

Fig. 6. (a) RAI surrounding the point indicated by an arrow in Fig. 2 ( $K = 2.1834$ ); the region  $(x_1, x_2)/(2\pi) \times (p_1, p_2)/(2\pi)$  covered by the graph is  $(0.09694, 0.097165) \times (-5.5 \cdot 10^{-5}, 5.5 \cdot 10^{-5})$ . (b) RAI surrounding point 1 in Fig. 3 ( $K = 8.68$ ), graph region is  $(0.9582, 0.9592) \times (0.674, 0.68)$ . (c) RAI surrounding point 2 in Fig. 4 ( $K = 8.916$ ), graph region is  $(0.019943, 0.0199537) \times (0.085314, 0.085334)$ . (d) RAI surrounding point 1 in Fig. 5 ( $K = 15.24035$ ), graph region is  $(0.97312, 0.97326) \times (0.7019, 0.704)$ .

Fig. 7. Plot of  $D_{\mathcal{E},t}(K)/D_{\text{ql}}$  for  $t = 500$  and  $K \in (1, 2\pi)$  ( $\Delta K = 5 \cdot 10^{-3}$ ), where  $D_{\text{ql}} = K^2/4$  is the quasilinear diffusion coefficient. The ensemble  $\mathcal{E}$  consists of the points  $(x_0, p_0)$  with  $p_0 = 0$  and  $x_0$  taking 20000 values uniformly distributed in  $[0, 2\pi)$ . The peaks indicated by arrows correspond to the RAIs no. 1, 3, 9, and 12 in Table I and were produced using  $t = 20000$  iterations and a finer grid in both  $K$  and  $x_0$ .

Fig. 8. Solid lines: Resonances 0/1 and 1/2 for  $K = 2.975$ . Shown is the RAI chain no. 7 in Table I, labeled by the time index  $t = 1, \dots, 4$ . A magnification of island no. 1 appears in the inset, showing strong stickiness of chaotic orbits to the RAI boundary.

Fig. 9. Solid line: Log-log plot of  $\langle p_t^2 \rangle_{\mathcal{E}}$  for  $K = 2.975$  (see more details in the text). Dashed line: Linear fit to the solid line, with slope  $\mu \approx 1.28$ .

Fig. 10. Time evolution of  $\langle p_t - p_0 \rangle_{\mathcal{E}}/(2\pi)$ , where  $\mathcal{E}$  is an ensemble of chaotic initial conditions (ICs)  $(x_0, p_0)$  extracted from a grid covering the graph region specified in the caption of: (a) Fig. 6(b) (19276 chaotic ICs out of 26867),  $K = 8.68$ ; (b) Fig. 6(c) (15639 chaotic ICs out of 21600),  $K = 8.916$ ; (c) Fig. 6(d) (10693 chaotic ICs out of 11788),  $K = 15.24035$ . The inset in (a), (b), and (c) shows a magnification of the first iterates with average slope  $\sim w/n = 1/2, 1/3, \text{ and } 1$ , respectively. The steplike structure due to the stickiness to the boundaries of the pure RAIs is quite evident in all cases.



This figure "fig1.gif" is available in "gif" format from:

<http://arxiv.org/ps/nlin/0612054v1>

This figure "fig2.gif" is available in "gif" format from:

<http://arxiv.org/ps/nlin/0612054v1>

This figure "fig3.gif" is available in "gif" format from:

<http://arxiv.org/ps/nlin/0612054v1>

This figure "fig4.gif" is available in "gif" format from:

<http://arxiv.org/ps/nlin/0612054v1>

This figure "fig5.gif" is available in "gif" format from:

<http://arxiv.org/ps/nlin/0612054v1>

This figure "fig6a.gif" is available in "gif" format from:

<http://arxiv.org/ps/nlin/0612054v1>

This figure "fig6b.gif" is available in "gif" format from:

<http://arxiv.org/ps/nlin/0612054v1>

This figure "fig6c.gif" is available in "gif" format from:

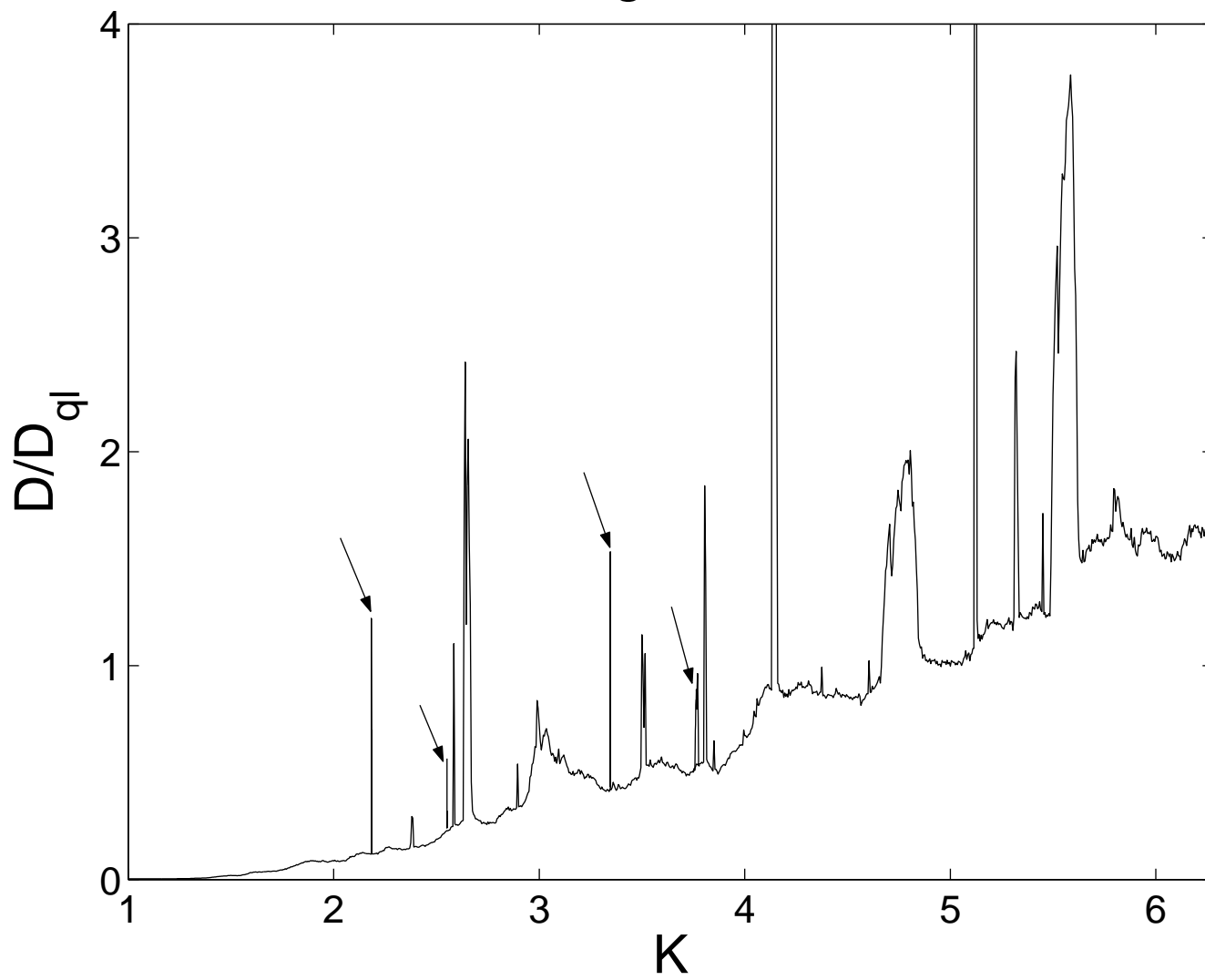
<http://arxiv.org/ps/nlin/0612054v1>



This figure "fig6d.gif" is available in "gif" format from:

<http://arxiv.org/ps/nlin/0612054v1>

Figure 7



This figure "fig8.gif" is available in "gif" format from:

<http://arxiv.org/ps/nlin/0612054v1>

Figure 9

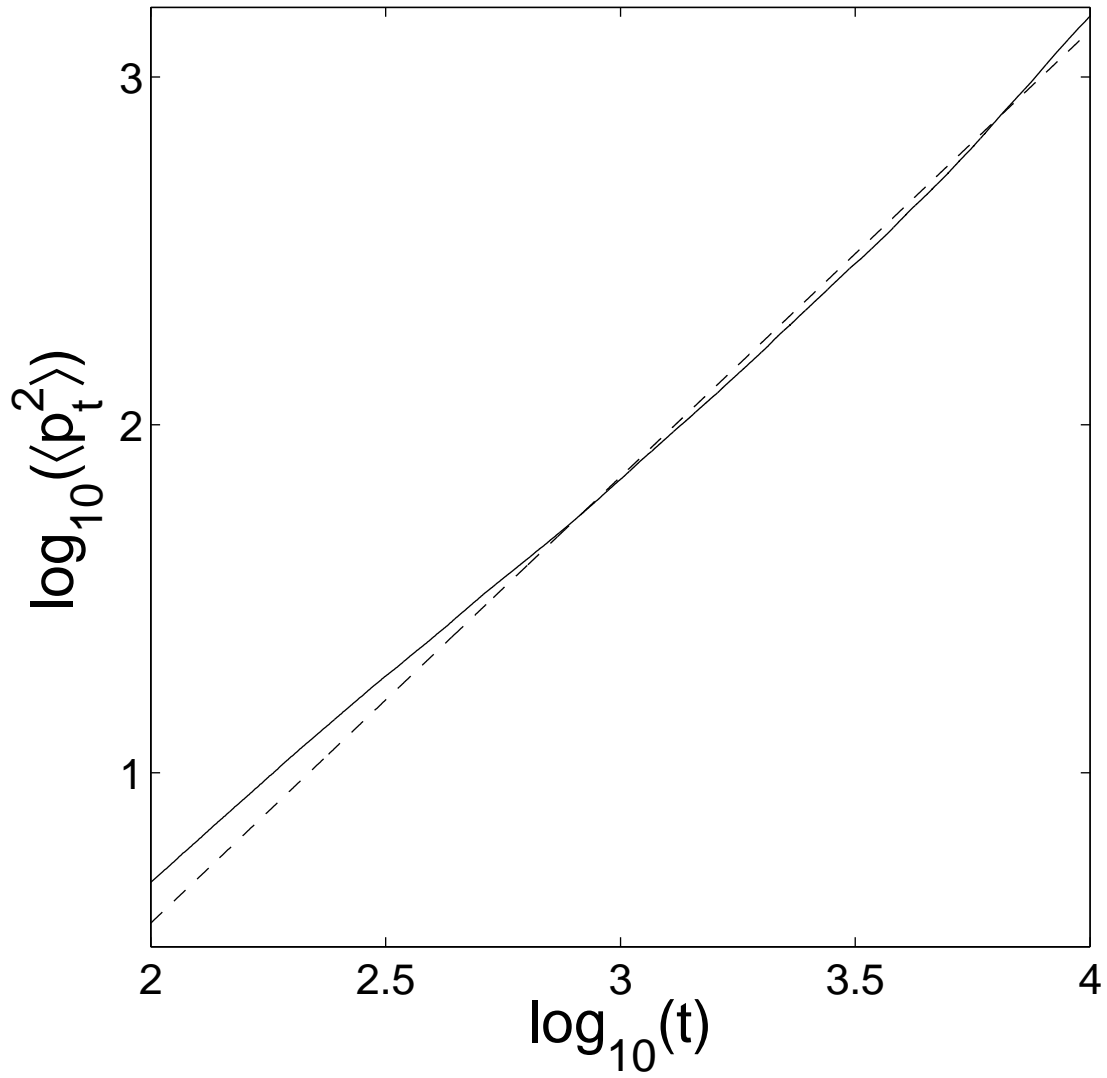


Figure 10(a)

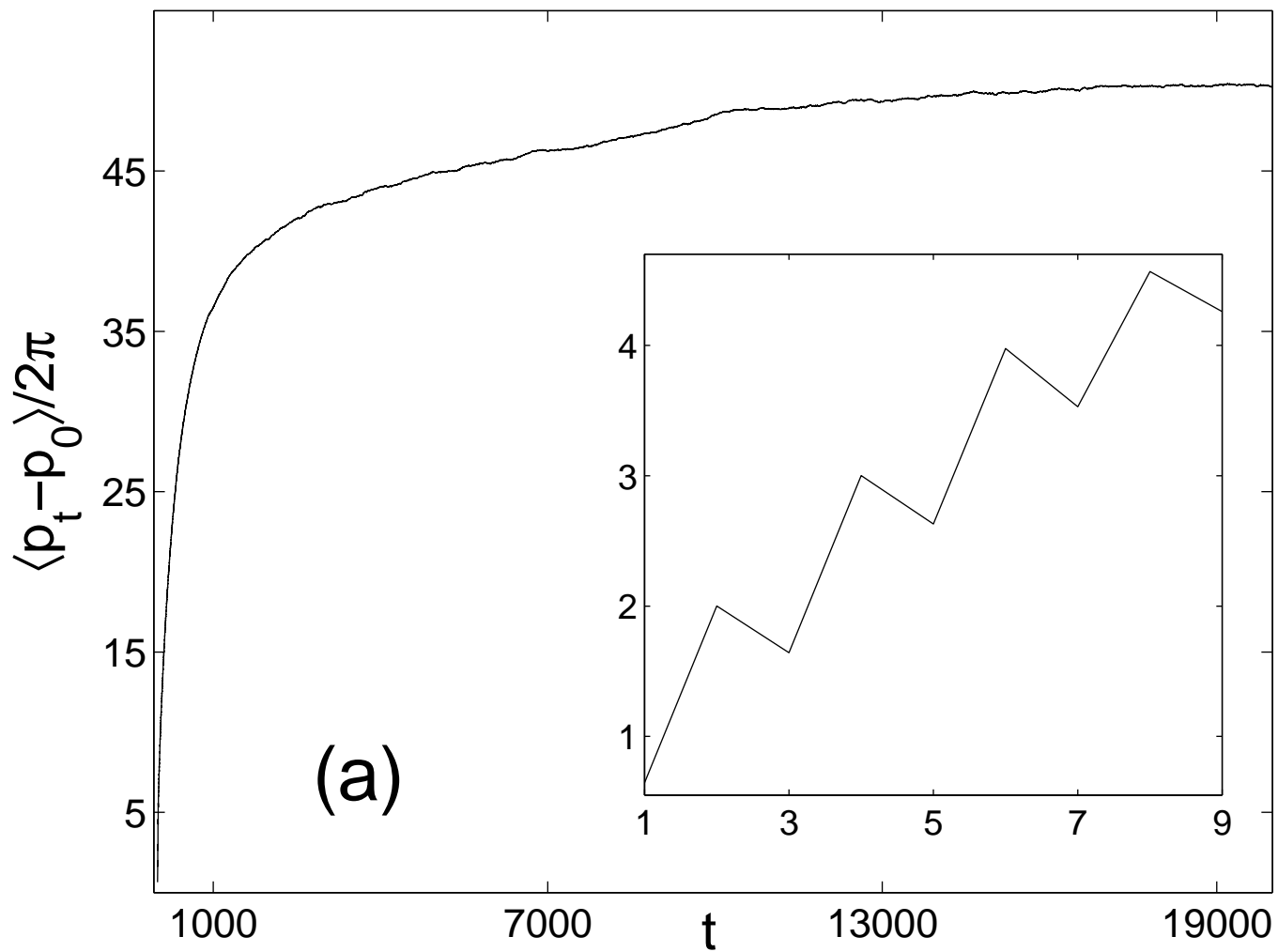


Figure 10(b)

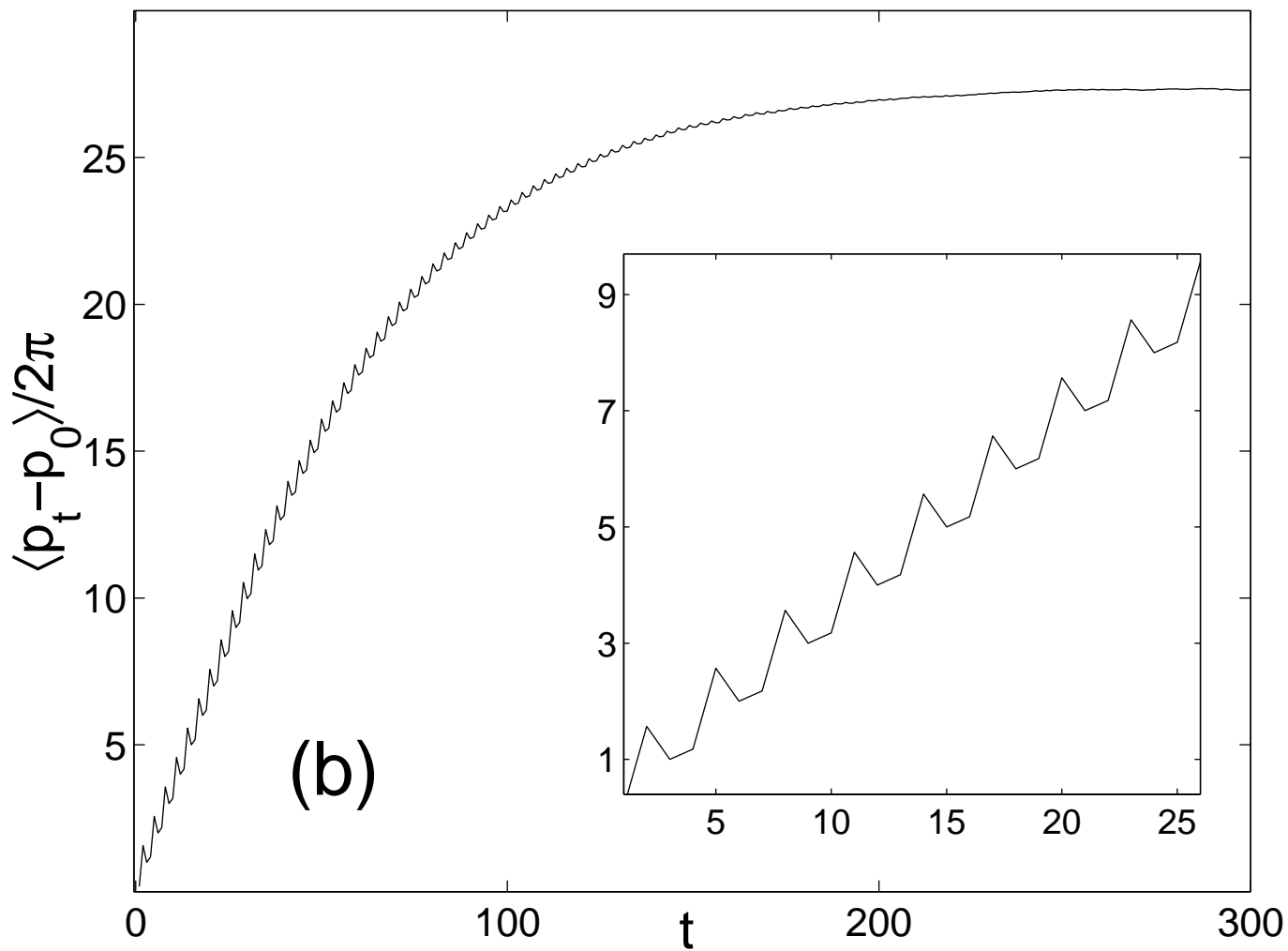


Figure 10(c)

